BILINGUAL PUBLISHING CO.
Pioneer of Global Academics Since 1984

Journal of Geographical Research
http://ojs.bilpublishing.com/index.php/jgr

REVIEW

A Review of Landsat TM/ETM based Vegetation Indices as Applied to Wetland Ecosystems

Gema Marco Dos Santos Ignacio Meléndez-Pastor Jose Navarro-Pedreño*
Ignacio Gómez Lucas

Departamento de Agroquímica y Medio Ambiente. Universidad Miguel Hernández de Elche. Av. Universidad, s/n. E-03202. Elche, Spain

ARTICLE INFO

Article history
Received: 23 January 2019
Accepted: 18 February 2019
Published: 5 March 2019

Keywords:
Biomass
Greenness
Leaf reflectance
NDVI
SAVI
Semi-arid environments

ABSTRACT

A review of vegetation indices as applied to Landsat-TM and ETM+ multispectral data is presented. The review focuses on indices that have been developed to produce biophysical information about vegetation biomass/greenness, moisture and pigments. In addition, a set of biomass/greenness and moisture content indices are tested in a Mediterranean semiarid wetland environment to determine their appropriateness and potential for carrying redundant information. The results indicate that most vegetation indices used for biomass/greenness mapping produce similar information and are statistically well correlated.

1. Introduction

In the last decades a broad range of vegetation indices has been developed, showing an increased interest by the scientific community in measuring vegetation properties through remote sensing techniques. A great number of indices are developed with the aim to reduce their sensitivity to extraneous factors such as soil background or atmosphere [1], and several reviews of vegetation indices have been published [2-7].

Remote sensing tools are used for a large number of studies of natural areas [8,9], to assess the state of vegetation or crop yield [10], or for vegetation classification [11]. In addition, several authors [12,13] have highlighted the role of vegetation indices as valuable biophysical data for models and simulations.

This work focuses on three biophysical properties, which are vegetation biomass/greenness, vegetation moisture, and plant pigments. Remote sensing of vegetation biomass is of great value in modelling vegetation stress and crop yield [14]. Numerous researches have shown the direct relationship that exists between spectral response in the near-infrared region and various biomass measurements [15-19]. Spatial and temporal change of vegetation

**Corresponding Author:*
Jose Navarro-Pedreño
Departamento de Agroquímica y Medio Ambiente. Universidad Miguel Hernández de Elche. Av. Universidad, s/n. E-03202. Elche, Spain.
Email: jonavar@umh.es

 DOI: https://doi.org/ 10.30564/jgr.v2i1.499

moisture can be used for plant water stress estimations. Water stress detection by remote sensing as based on plant physiology can be successfully conduced for different vegetation types with little adjustment [20-22]. A great number of research work has been conducted for estimating vegetation moisture content [6, 21-23] with a common goal: vegetation moisture content can be estimated more accurately using medium-infrared reflectance data. Chrolophylls, carotenoids and anthocyanins are optically detectable and have either photosynthetic or photoprotective functions [24]. Moreover, they also provide an accessible 'handle' for evaluating relative photosynthetic activity, which can vary with leaf type [25]. Reflectance assessment of leaf pigments can potentially provide indicators of integrated leaf physiology under a wide range of conditions [24]. For quantitative pigment content estimations, accurate data calibration methods must be carefully applied. As Gamon and Surfus (1999) [24] observed, comparisons of reflectance indices with extracted pigment levels suggest specie-specific relationships influenced by leaf structure properties [26]. This indicates a need for empirical calibration when using reflectance indices.

A great number of studies deal with vegetation index estimations for specific locations. These kinds of studies are of great value for these local studies, because vegetation indices can be estimated with great accuracy. In addition, due to the high availability of images, it is possible to monitor the state of the vegetation over time [27]. However, applying these locally tested methods to other study areas is sometimes not possible because of the different vegetation species and communities, as well as the different soils and lithology encountered in other areas.

The objective of this paper is the review of several vegetation indices that can be computed with Landsat TM and ETM+ data in order to select the most representative of the Mediterranean wetland areas by first determining potentially redundant information among the tested indices.

2. Vegetation Indices

Jensen (2000) [4] defines vegetation indices as "dimensionless, radiometric measures that function as indicators of relative abundance and activity of green vegetation, often including leaf-area-index (LAI), percentage green cover, chlorophyll content, green biomass, and absorbed photosynthetically active radiation (APAR)". Huete and Justice (1999) [28] summarize as follows the main characteristics that a vegetation index must satisfy:

1) Maximize sensitivity to plant biophysical parameters, with mathematical relations as simple as possible.

2) Normalize or model external effects, such as Sun angle, scene geometry, and space-temporal atmospheric characteristics.

3) Normalize internal effects, such as canopy and soil background variations, illumination geometry, and phenological state.

4) Respond to specific measurable biophysical parameters, such as biomass, LAI, APAR, etc., that can be field validated and qualitatively controlled.

Vegetation spectral indices try to enhance the spectral contrast among different wavelengths as a response to characteristic absorption and/or reflectance features. A crucial aspect is that the absorptions from different plant materials are similar and overlap, so that a single absorption band cannot be isolated and directly related to, for example, chemical abundances of one plant constituent [29]. Vegetation indices have been classified into four categories as a function of the following computation concepts (based partially on: Jackson and Huete (1991) [30] and Eastman (2003) [31]):

1) Slope-based indices: any particular value of the index can be produced by a set of two bands (for example red/infrared reflectance values) that form a line emanating from the origin of coordinates of a bi-spectral plot (scattergram). Different levels of the index can be envisioned as producing a spectrum of such lines that differ in their slope [32].

2) Distance-based indices: measure the degree of vegetation present by gauging the difference of any pixel's reflectance from the reflectance of bare soil [32]. A key concept here is that a plot of the positions of bare soil pixels of varying moisture levels (and soil organic matter contents [33] in a bi-spectral plot will tend to form a line (known as the soil line). As vegetation canopy cover increases, this soil background will become progressively obscured, with vegetated pixels showing a tendency towards increasing along a perpendicular distance from this soil line. All of the members of this group require that the slope and intercept of the soil line be defined for the particular image being analysed.

3) Orthogonal transformations: undertake a transformation of the available spectral bands to form a new set of uncorrelated bands within which a green vegetation index band can be defined.

4) Continuum Removal and Band Depth: the continuum is an estimate of the other absorptions present in the spectrum, not including the one of interest [33]. The continuum-removal process isolates spectral features, removes the continuum, and scales the band-depth (or band area) to be equal, to allow identification of subtle band shifts and shapes [34].

DOI: https://doi.org/ 10.30564/jgr.v2i1.499

Table 1 provides a classification of the indices as a function of the calculation concept. All presented indices have been adapted so that they can be utilized with reflectance imagery provided by the Landsat Thematic Mapper sensor.

Technical information about the Thematic Mapper sensor can be found at the U.S. Geological Survey Landsat Project web site (http://landsat.usgs.gov).

Table 1. A classification of the indices as a function of the calculation concept

Index computation concept	Index
Slope-based	SR NDVI TVI OSAVI ARVI NDII LWCI MSI Red/Green ratio WDVI
Distance-based	PVI SAVI MSAVI TSAVI1 TSAVI2 GESAVI SARVI MSARVI EVI
Orthogonal transformation	Tasseled Cap-Greenness Tasseled Cap-Wetness Integral
Continuum Removal and Band Depth	Band-Depth TM5 (B-DTM5)

2.1 Slope-based Indices

Generally, slope-based indices are easier to calculate than other indices. Some indices are normalized ratios where possible results are comprised between the range of −1 to 1. This approach facilitates the interpretation of the index.

2.1.1 Normalized Difference Vegetation Index (NDVI)

NDVI original formulation is attributed to Rouse et al. (1974) [35]. This index has been widely used and tries to enhance reflectance differences between red and NIR spectral regions of plant spectral signatures. The NDVI index evolved from the Simple Ratio (SR) proposed by Birth and McVey (1968) [36].

$$SR = \frac{\rho_{TM4}}{\rho_{TM3}} \tag{1}$$

The NDVI is formulated as:

$$NDVI = \frac{\rho_{M4} - \rho_{M3}}{\rho_{M4} + \rho_{M3}} \tag{2}$$

Deering et al. (1975) [37] proposed the Transformed Vegetation Index (TVI) by adding a constant value of 0.5 to the NDVI to avoid negative values. They also included the square root transformation of the NDVI with the additional constant, to stabilize the variance. TVI is computed as:

$$TVI = \sqrt{\left(\frac{\rho_{M4} - \rho_{M3}}{\rho_{M4} + \rho_{M3}}\right) + 0.5} \tag{3}$$

NDVI has been related with a great number of parameters, such as changes in the amount of green biomass and chlorophyll content [4]. Several types of relationships with numerous parameters have been reported. A synthetic summary of some of them is presented below ([38] and references therein):

a. Leaf chlorophyll content
b. Leaf water content
c. CO_2 net flux
d. Absorbed Photosynthetically Active Radiation (APAR)
e. Vegetation net productivity
f. Leaf Area Index (LAI)
g. Rainfall amount received by a vegetation canopy
h. Phenological dynamics
i. Potential plant transpiration

2.1.2 Optimized Soil-Adjusted Vegetation Index (OSAVI)

Additional modifications of NDVI have been developed to minimize the effect of soil background and atmospheric attenuation for the maximization of vegetation spectral response. Rondeaux et al. (1996) [39] proposed the OSAVI (Optimized Soil-Adjusted Vegetation Index) with the inclusion of an adjusting factor X to the NDVI denominator. They estimated, using the SAIL model [40] enhanced by the hot-spot effect [41], that the optimum X value was 0.16 units. OSAVI values range between the NDVI and SAVI estimations.

$$OSAVI = \frac{\rho_{TM4} - \rho_{TM3}}{\rho_{TM4} + \rho_{TM3} + 0.} \tag{4}$$

Rondeaux et al. (1996) [39] also provided a test of the sensitivity to soil background for many vegetation indi-

 DOI: https://doi.org/ 10.30564/jgr.v2i1.499

ces. They evaluated the sensitivity of OSAVI to soil background effects and its relationship with NDVI and SAVI [42,43]. They concluded that: a) with low or relative low vegetation cover (< 50%, LAI ≤ 1) this index performs slightly worse than SAVI but better than NDVI; b) with high or relative high vegetation cover, (<50%, LAI ≥ 1) the index performs slightly worse than NDVI but better than SAVI. Steven (1998) [44] evaluated the OSAVI with a canopy model to observational parameters and concluded that the index can be used successfully for agricultural monitoring.

2.1.3 Atmospherically Resistant Vegetation Index (ARVI)

ARVI was proposed by Kaufman and Tanre (1992) [45]. The index tries to minimize atmospheric effects (molecular scattering and ozone absorption) due to the normalization of the blue, red, and near-infrared reflectance bands. Kaufman and Tanre (1992) [45] indicated that atmospheric aerosol influences vegetation indices in two ways[28]:

1) Influence as path radiance: By an additive, effect due to land surface brightness.

2) Influence through transmittance: By a multiplicative, effect due to surface

brightness.

The ARVI uses blue band to reduce atmospheric effects in the red band, by using an experimental aerosol model (γ). Kaufman and Tanre (1992) [45] provided guidelines for aerosol model values selection. γ is normally equal to 1 to minimize atmospheric effects.

$$ARVI = \frac{\rho^*_{TM4} - \rho^*_{rb}}{\rho^*_{TM4} + \rho^*_{rb}} \quad (5)$$

$$\rho^*_{rb} = \rho^*_{TM3} - \gamma\left(\rho^*_{TM1} - \rho^*_{TM3}\right) \quad (6)$$

where:

ρ^*_k = apparent reflectance of band k

γ = aerosol model

ARVI is similar to NDVI with respect to potentially related biophysical parameters.

2.1.4 Normalized Difference Infrared Index (NDII)

The original Infrared Index (II) was proposed by Hardisky et al. (1983) [46] and was cited by Hunt and Rock (1989) [22] as Normalized Difference Infrared Index (NDII). NDII differs from NDVI in that TM band 3 (red spectral region) is replaced by band 5 (mid-infrared spectral region). TM band 5 can be related with a leaf water absorption band [4]. Carter (1991) [47] showed that mid-infrared reflectance increases are related with decreases in plant moisture.

$$NDII = \frac{\rho_{TM4} - \rho_{TM5}}{\rho_{TM4} + \rho_{TM5}} \quad (7)$$

NDII is highly correlated with canopy water content [46]. Jensen (2000) [4] highlighted that NDII is more sensitive to changes in plant biomass and water stress than NDVI in wetland studies. Several studies have shown that these kinds of indices that combines near-infrared with mid-infrared bands is more appropriate than NDVI for estimating vegetation water contents [6,23,48].

A similar index to NDII is the Leaf Water Content Index (LWCI) proposed by Hunt et al. (1987) [21] for leaf Relative Water Content (RWC) estimations. It is based on the principle that, according to Beer's law, absorbance of infrared radiation by leaf water (A) is equal to the product of the equivalent water thickness (l), the extinction coefficient (ε_w), and the concentration of water (c_w, [21] computed it as 55.6 mol/L). The ratio of leaf absorbance to leaf absorbance at full turgor (A/A_{FT}) is equal to the ratio of equivalent thickness (l/l_{FT}) because ε_w and c_w cancel out. Consequently, A/A_{FT} is equal to the ratio of water volumes averaged over the leaf area (V/V_{FT}), which is RWC.

$$LWCI = \frac{-\log\left[1-(\rho_{TM4} - \rho_{TM5})\right]}{-\log\left[1-(\rho_{TM4FT} - \rho_{TM5FT})\right]} \quad (8)$$

where:

$\rho_{TM_k FT}$ = reflectance of TM band k when leaves area at full turgor

Hunt and Rock (1989) [22] reported that LWCI can measure leaf RWC directly and is useful to determine when certain plants are water stressed. However, the required reflectance measurements and two different but known RWC make it impractical for field applications.

2.1.5 Red/Green Ratio

This index was proposed by Gamon and Surfus (1999) [24] to assess anthocyanin content. The role of this kind of plant pigment is unclear [24]: being both photoprotective [50] and defensive [51,52]. Gamon and Surfus (1999) [24] suggested the possible role of anthocianyns: "the complementary patterns of xanthophyll and anthocyanin pigmentation during early leaf development suggest that anthocianyns provide a critical, photoprotective role before xanthophylls pigments reach final levels" (not fully developed photosyn-

DOI: https://doi.org/ 10.30564/jgr.v2i1.499

thetic competence). The index is formulated as:

$$R/G = \frac{\rho_{TM3}}{\rho_{TM2}} \quad (9)$$

Gamon and Surfus (1999) [24] observed that the Red/Green ratio was strongly related to anthocyanin pigment content estimated by destructive sampling and spectrophotometric quantification.

2.2 Distance-based Indices

A key concept for distance-based vegetation indices is the soil line. Richardson and Wiegand (1977) [53] discovered the concept of the soil line. It results from a linear relationship between the red and near-infrared reflectance values of bare soils:

$$y = ax + b \quad (10)$$

where:
x = reflectance of red band
y = reflectance of near-infrared band
a = slope of the soil line
b = intercept of the soil line

The soil line is dependent on individual soil types. Fox et al., (2004) [54] affirmed that a global soil line representing all soil types is not possible due to the fact that the line would be linear in some portions of the entire range as a result of soil condition variations (soil type, moisture, organic matter content, etc.).

The original index for this group is the Perpendicular Vegetation Index (PVI) proposed by Richardson and Wiegand (1977) [53]. The derivation of the index requires several steps (based on Eastman, 2003 [31]):

A. Determination of the soil line equation by bare soil reflectance values for red (independent variable) vs. infrared (dependent variable) bands.

$$\rho_{g4} = a \cdot \rho_{g3} + b \quad (11)$$

where:
ρ_{g3} = an x position on the soil line
ρ_{g4} = the corresponding y coordinate
a = the slope of the soil line
b = the y-intercept of the soil line

B. Determine the equation of the line that is perpendicular to the soil line, with the form:

$$\rho_{p4} = c \cdot \rho_{p3} + d \quad (12)$$

where:
ρ_{p3} = red reflectance
ρ_{p4} = infrared reflectance
c = -1/a
$d = \rho_{p4} - c \cdot \rho_{p3}$

C. Find the intersection of the two lines (i.e., the coordinate ρ_{gg3}, ρ_{gg4}).

$$\rho_{gg4} = \frac{c \cdot b - d\ a}{c - a} \quad (13)$$

$$\rho_{gg3} = \frac{b - d}{c - a} \quad (14)$$

D. Find the distance between the intersection and the pixel coordinate using Pythagoras' Theorem.

$$PVI = (\sqrt{\left(\rho_{gg4} - \rho_{gg4}\right)^2 + \left(\rho_{gg3} - \rho_{gg3}\right)^2} \quad (15)$$

2.2.1 Soil Adjusted Vegetation Index (SAVI)

SAVI results from a modification of NDVI by the addition of a soil adjustment factor (L)[42,43]. L value varies as a function of soil characteristics. The index is formulated as:

$$SAVI = \frac{(\rho_{TM4} - \rho_{TM3})}{(\rho_{TM4} + \rho_{TM3} + L)}(1 + L) \quad (16)$$

where:
L = soil adjustment factor

Originally, a graphical method was used for L value extraction. If L = 0, SAVI = NDVI, and if L = 100, SAVI ≅ PVI. Huete (1988) [42] suggested an L value of 1 for areas with low vegetation, L value of 0.5 for intermediate areas, and L value of 0.25 for densely vegetated areas. SAVI is similar to NDVI with respect to potentially related biophysical parameters.

Qi et al. (1994) [52] developed the MSAVI (Modified Soil Adjusted Vegetation Index) with the inclusion of a new L adjustment factor that considers the soil line, the NDVI and the WDVI (Weighted Difference Vegetation Index) [55, 56]. The new L factor is formulated as:

$$L = 1 - 2 \cdot a \cdot NDVI \cdot WDVI \quad (17)$$

where:

$$WDVI = \rho_{TM4} - a \cdot \rho_{TM3} \quad (18)$$

 DOI: https://doi.org/ 10.30564/jgr.v2i1.499

and:

a = slope of the soil line (for L and WDVI)

They proposed two formulations to the MSAVI, the first is identical to the original SAVI but with the new L soil adjustement factor, and the last one is as follows:

$$MSAVI = \frac{2 \cdot \rho_{TM4} + 1 - \sqrt{(2 \cdot \rho_{TM4} + 1)^2 - 8 \cdot (\rho_{TM4} - \rho_{TM3})}}{2} \quad (19)$$

2.2.2 Transformed Soil Adjusted Vegetation Index (TSAVI)

Baret et al. (1989) [57] argued that SAVI was only valuable if the soil line constants are a=1 and b=0. They developed the first modification of SAVI, the TSAVI1, which is formulated as:

$$TSAVI_1 = \frac{a \cdot ((\rho_{TM4} - a) \cdot (\rho_{TM3} - b))}{\rho_{TM3} + a \cdot \rho_{TM4} - a \cdot b} \quad (20)$$

where:

a = slope of the soil line

b = intercept of the soil line

TSAVI1 tries to combine the potentials of SAVI and PVI. The problem of TSAVI1 is that the index does not give good results in areas of heavy vegetation, because it is designed for semiarid areas. Baret et al. (1991) [57] proposed a modification of the first TSAVI. The TSAVI2 included a correction factor of 0.08 to minimize soil brightness background effects.

$$TSAVI_2 = \frac{a \cdot (\rho_{TM4} - a \cdot \rho_{TM3} - b))}{\rho_{TM3} + a \cdot \rho_{TM4} - a \cdot b + 0.08 \cdot (1 + a^2)} \quad (21)$$

where:

a = slope of the soil line

b = intercept of the soil line

2.2.3 Generalized Soil-Adjusted Vegetation Index (GESAVI)

Gilabert et al. (2002) [58] used the concept of vegetation isolines for the development of the Generalized Soil-Adjusted Vegetation Index (GESAVI), an index that belongs to the SAVI family. The index is based on the angular distance between the soil line and the vegetation isolines. They assume that vegetation isolines are linear but not parallel to the soil line, and the soil line is intercepted by the vegetation isolines at a cross point with a given red reflectance equal to:

$$R_{cross} = -\frac{b' - b}{a' - a} \quad (22)$$

where:

a = slope of the soil line

a' = slope of the vegetation isoline

b = intercept of the soil line

b' = intercept of the vegetation isoline

They also provided a geometrical interpretation of the index. The index is formulated as:

$$GESAVI = \frac{\rho_{TM4} - a \cdot \rho_{TM3} - b}{\rho_{TM3} + Z} \quad (23)$$

where:

$Z \equiv - R_{cross}$

2.2.4 Soil and Atmospherically Resistant Vegetation Index (SARVI)

SARVI results from the integration of the soil adjustment factor (L) of SAVI with the normalization of the blue, red, and near-infrared reflectance bands of ARVI [59]. The index is formulated as:

$$SARVI = \frac{\rho^*_{TM4} - \rho^*_{rb}}{\rho^*_{TM4} + \rho^*_{rb} + L} \quad (24)$$

$$\rho^*_{rb} = \rho^*_{TM3} - \gamma \cdot (\rho^*_{TM1} - \rho^*_{TM3}) \quad (25)$$

where:

ρ^*_k false= apparent reflectance of band k

L = soil adjustment factor

γ = aerosol model

Huete and Liu (1994) [59] also proposed the MSARVI, a modification of SARVI.

$$MSARVI = \frac{2 \cdot \rho^*_{TM4} + 1 - \sqrt{\left[\left(2 \cdot \rho^*_{TM4} + 1\right)^2 - \gamma \cdot \left(\rho^*_{TM4} - \rho^*_{rb}\right)\right]}}{2} \quad (26)$$

$$\rho^*_{rb} = \rho^*_{TM3} - \gamma \cdot \left(\rho^*_{TM1} - \rho^*_{TM3}\right) \quad (27)$$

where:

ρ^*_k false= apparent reflectance of band k

L = soil adjustment factor

γ = aerosol model

Huete and Liu (1994) [59] provided a sensitivity analysis of SAVI, ARVI, SARVI, and MSARVI with respect to NDVI. Jensen (2000) [4] reports several cases:

DOI: https://doi.org/ 10.30564/jgr.v2i1.499

Case 1. Only soil noise (total atmospheric correction): SAVI and MSARVI are the best indices, and NDVI and ARVI are the worst.

Case 2. Partial atmospheric correction (Rayleigh and ozone components removed): SARVI and MSARVI are the best indices, and NDVI and ARVI are the worst.

Case 3. No atmospheric correction: SARVI are the best index, and NDVI and ARVI are the worst.

2.2.5 Enhanced Vegetation Index (EVI)

The EVI was developed by Huete and Justice (1999) [28] based on the MODIS sensor as an index with "improved sensitivity into high biomass regions and improved vegetation monitoring through a de-coupling of the canopy background signal and a reduction in atmosphere influences". EVI is formulated as:

$$EVI = \frac{\rho^*_{TM4} - \rho^*_{TM3}}{\rho^*_{TM4} + C_1 \cdot \rho^*_{TM3} - C_2 \cdot \rho^*_{TM1} + L} \cdot (1 + L) \quad (28)$$

where:

ρ^*_k false= apparent reflectance of band k

L = soil adjustment factor

C_1, C_2 = use of the blue band in correction of the red band for atmospheric aerosol scattering.

EVI has been formulated for global vegetation studies and for the improvement in the extraction of canopy biophysical parameters. EVI application to global MODIS data is accessible as part of the NASA-Earth Observing System (EOS) program.

2.3 Orthogonal Transformations

The derivation of orthogonal transformation indices is complicated. Principal Component Analysis can be considered as a reference point for orthogonal transformation indices. Selected indices are:

2.3.1 Tasseled Cap Transformation

Kauth and Thomas (1976) [60] derived an orthogonal transformation with four components from original Landsat MSS data. They used an imagery repository of an agricultural area, and tried to make a synthesis of crops spectral variation axes. They obtained a 3-D figure, the 'Tasseled Cap'. The four components that Kauth and Thomas calculated, are soil brightness (B), vegetation greenness (G), yellow stuff (Y), and non-such (N):

$$B = 0.332 \cdot \rho_{mms1} + 0.603 \cdot \rho_{mms2} + 0.675 \cdot \rho_{mms3} + 0.262 \cdot \rho_{mms4} \quad (29)$$

$$G = -0.283 \cdot \rho_{mms1} - 0.6 \cdot \rho_{mms2} + 0.577 \cdot \rho_{mms3} + 0.388 \cdot \rho_{mms4} \quad (30)$$

$$Y = -0.899 \cdot \rho_{mms1} + 0.428 \cdot \rho_{mms2} + 0.076 \cdot \rho_{mms3} - 0.041 \cdot \rho_{mms4} \quad (31)$$

$$N = -0.016 \cdot \rho_{mms1} + 0.131 \cdot \rho_{mms2} - 0.452 \cdot \rho_{mms3} + 0.882 \cdot \rho_{mms4} \quad (32)$$

Crist (1985) [61] derived computed Tasseled Cap components for TM data. He derived three components, brightness (B), greenness (G), and wetness (W).

$$B = 0.0243 \cdot \rho_{TM1} + 0.4158 \cdot \rho_{TM2} + 0.5524 \cdot \rho_{TM3} + 0.5741 \cdot \rho_{TM4} + 0.3124 \cdot \rho_{TM5} - 0.2303 \cdot \rho_{TM7} \quad (33)$$

$$G = -0.1603 \cdot \rho_{TM1} - 0.2819 \cdot \rho_{TM2} - 0.4939 \cdot \rho_{TM3} + 0.794 \cdot \rho_{TM4} - 0.0002 \cdot \rho_{TM5} - 0.1446 \cdot \rho_{TM7} \quad (34)$$

$$W = 0.0315 \cdot \rho_{TM1} + 0.2021 \cdot \rho_{TM2} + 0.3102 \cdot \rho_{TM3} + 0.1594 \cdot \rho_{TM4} - 0.6806 \cdot \rho_{TM5} - 0.6109 \cdot \rho_{TM7} \quad (35)$$

TM brightness component is related with total reflectivity of the scene, the greenness component can be related with the concept of NDVI, and the wetness component is related with plant moisture [4,6]. A great amount of research work has been focused on the Tasseled Cap transformation concept [62-65]. For the computation of Tasseled Cap coefficients to local condition and for various sensors, Jackson (1983) [66] provides useful guidelines.

2.3.2 Integral

The basis of this index relies on the absorption effect of water on visible and SWIR bands. The index has been developed in the framework of forest fires research [6]. Integral is computed as:

$$Integal = 0.07 \cdot \rho_{TM1} + 0.08 \cdot \rho_{TM2} + 0.06 \cdot \rho_{TM3} + 0.2 \cdot \rho_{TM5} + 0.27 \cdot \rho_{TM7} \quad (36)$$

Integral is negatively related with Fuel Moisture Content (FMC). Chuvieco et al. (2002)[6] do not consider the near-infrared band to avoid indirect effects (LAI, grass curing) on FMC estimation.

2.4 Continuum Removal and Band Depth

Clark and Roush (1984) [67] established the bases of the Continuum Removal concept. This technique can be considered as the core of Imaging Spectroscopy. Absorptions in a spectrum have two components [67,68]:

• Continuum: is the 'background absorption' onto which other absorption features are superimposed.

• Individual features: attributed to individual components.

The depth of absorption can be related to the abundance of the absorber and the grain of the material [68]. By

 DOI: https://doi.org/ 10.30564/jgr.v2i1.499

searching specific absorption features for individual components (e.g. H_2O, Fe_2S, lignin), and calibrating data with other analytical methods (e.g. X-ray chromatography, HPLC), an accurate quantitative estimation of components can be done.

Clark et al. (2003) [69] indicated that the apparent depth of an absorption feature (D) relative to the surrounding continuum in a reflectance or emittance spectrum [67] is:

$$D = 1 - \frac{R_b}{R_c} \tag{37}$$

where:

Rb = reflectance of the absorption-band centre (minimum of the continuum-removed feature)

Rc = reflectance value of the continuum at the wavelength of the band centre

Adapted from Kokaly and Clark (1999) [29], Van Niel (2003) [70] provided equations for continuum-removed band depth analysis of vegetation moisture. They used a very simplified version of band depth analysis with only tree bands, TM4 and TM7 as respectively left and right extremes of the continuum, and TM5 as the absorption-band centre. As previously mentioned, TM band 5 can be related with a leaf water absorption band [4]. TM adapted continuum-removed band depth analysis equations are as follow:

$$D_{TM5} = 1 - R' \tag{38}$$

$$R' = \frac{\rho_{TM5}}{(\rho_{TM4} \cdot (1-c)) + (\rho_{TM7} \cdot c)} \tag{39}$$

$$c = \frac{\lambda_{TM5} - \lambda_{TM4}}{\lambda_{TM7} - \lambda_{TM4}} \approx 0.59359 \tag{40}$$

3. Test Site Example: Imagery and Pre-processing

The selected test site is located in the southeast coast of Spain, in Alicante (figure 1). With a Mediterranean climate (hot summers and warm winters), and a semi-arid rainfall regimen (mean annual rainfall lower than 300 mm), this test site is composed by a set of coastal wetlands surrounded by salt flats, agricultural and urban areas. These wetlands are included in the list of Ramsar sites and protected as Natural Parks (Salinas de Santa Pola and El Hondo in Crevillente-Elche). A key factor that characterizes these wetlands and their biodiversity is the electrical conductivity of the water bodies, ranging from 2.5 mS/cm, 10 mS/cm for salty waters to more than 220 mS/cm for hypersaline waters (in salt flats). Water inputs of these ecosystems are in the form of in situ rainfall, natural river basin runoff, agricultural channels, and seawater channels (for salt flats).

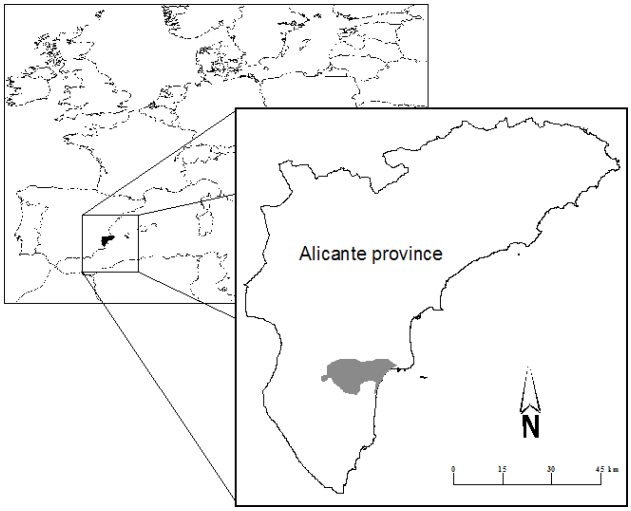

Figure 1. Test area (Ramsar wetland site) located in south-eastern coast of Spain, in Alicante province

A LANDSAT 5 Thematic Mapper scene (path 199, row 33, WRS-2) acquired on 14/08/2005 (10:31:49 a.m.) by ESA (European Space Agency) ground receiving station in Matera (Italy) was used for the analysis. TM bands 2, 3, and 4 covering the study site are shown in figure 2.

An image to map geometric correction using the bilinear function and nearest neighbour resampling method was performed [6,71] using high precision vectorial cartography obtained by digitalisation of aerial orthophotographies at 1 m spatial resolution. The RMS error of the geometrically corrected TM scene was less than half a pixel (13.84 m).

DOI: https://doi.org/ 10.30564/jgr.v2i1.499

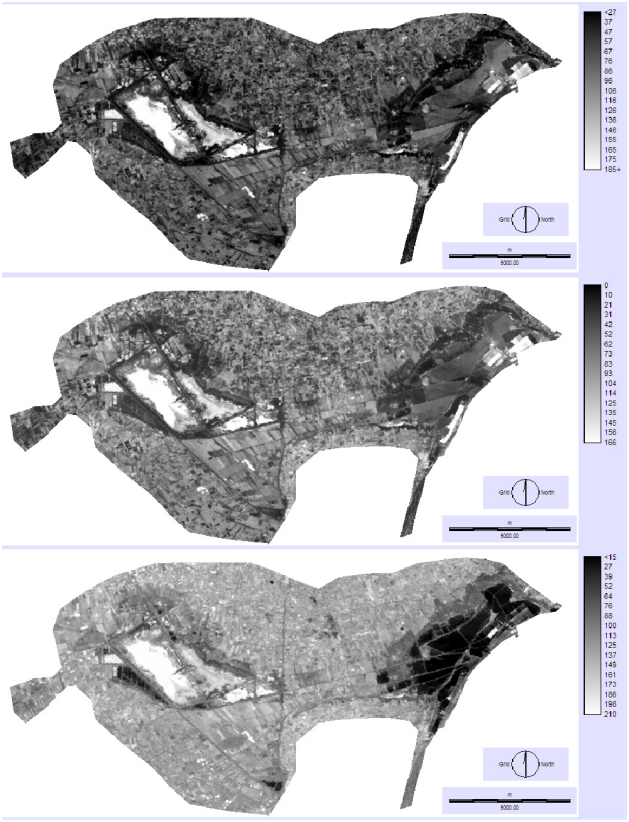

Figure 2. LANDSAT-TM bands 2, 3, and 4 (from top to bottom) shown as greyscale images of the test area. The image was acquired on 08/14/2005 for path 199, row 33 (WRS-2) by Landsat-5

Radiometric calibration of optical bands was carried out according to the guidelines reported by Chander and Markham (2003) [72] for the calculation of exoatmospheric reflectance. They defined two necessary steps. The first one is the conversion of calibrated digital numbers (Q_{cal}) to at-sensor spectral radiance (L_λ):

$$L_\lambda = \left(\frac{LMAX_\lambda - LMIN_\lambda}{Q_{cal\,\max}} \right) \cdot Q_{cal} + LMIN_\lambda \quad (41)$$

where:

L_λ = spectral radiance at the sensor's aperture ($W/m^2 \cdot sr \cdot \mu m$)

Q_{cal} = quantized calibrated pixel value in DNs

$Q_{cal\ max}$ = maximum quantized calibrated pixel value (DN = 255) corresponding to $LMAX_\lambda$

$LMIN_\lambda$ = spectral radiance as scaled to $Q_{cal\ min}$ in $W/(m^2 \cdot sr \cdot \mu m)$

$LMAX_\lambda$ = spectral radiance as scaled to $Q_{cal\ max}$ in $W/(m^2 \cdot sr \cdot \mu m)$

$LMAX_\lambda$ and $LMIN_\lambda$ values are provided by Chander and Markham [72]. The second step is the conversion from at-sensor radiance (L_λ) to exoatmospheric reflectance (ρ_P):

$$\rho_P = \frac{\pi \cdot L_\lambda \cdot d^2}{ESUN_\lambda \cdot \cos\theta_S} \quad (42)$$

where:

ρ_P = planetary or apparent reflectance

L_λ = spectral radiance at the sensor's aperture ($W/m^2 \cdot sr \cdot \mu m$)

d = Earth-Sun distance (A.U.)

$ESUN_\lambda$ = mean solar exoatmospheric irradiances

θ_S = solar zenith angle (degrees)

Chander and Markham [72] also list the $ESUN_\lambda$ and d values.

Because haze is the most important atmospheric attenuation element [73], a simple dark object subtraction by minimum value of histogram [71] was done in order to obtain an approximation of ground reflectance. Previous studies in Spain have used this atmospheric correction successfully[6,74,75].

In order to improve the visual interpretation of the results and the statistical analysis, a water body mask was built. A normalized ratio of TM bands 1 and 5 reflectance data was calculated based on the singularity of spectral characteristics of water bodies, which show higher reflectance values in the blue spectral region and lower reflectance values in the SWIR spectral region. This ratio was designed as the Normalized Water Bodies Surface Index (NWBSI) and the following formulation is proposed for TM bands based on the spectral characteristics of the water bodies:

$$NWBSI = \frac{\rho_{TM1} - \rho_{TM5}}{\rho_{TM1} + \rho_{TM5}} \quad (43)$$

The selection of TM band 5 as the band representing the SWIR spectral region is due to the occurrence of very intense water band absorption in soils and vegetation with very high moisture contents (typical in wetland ecosystems) in TM band 7 [76] which may generate some confusion. The thresholds selected for the discrimination of water bodies are: NDWSI > 0 for water bodies; NDWSI ≤ 0 for non-water bodies.

For distance-based indices, slope line calculation was done by extracting reflectance data at known bare soil areas. 1,013 pixels were used for the slope line regression analysis (figure 3). Slope coefficient (a = 1.0657) and interception coefficient (b = 0.1059) were calculated. A

 DOI: https://doi.org/ 10.30564/jgr.v2i1.499

correlation coefficient (r^2) of 0.915 was then obtained.

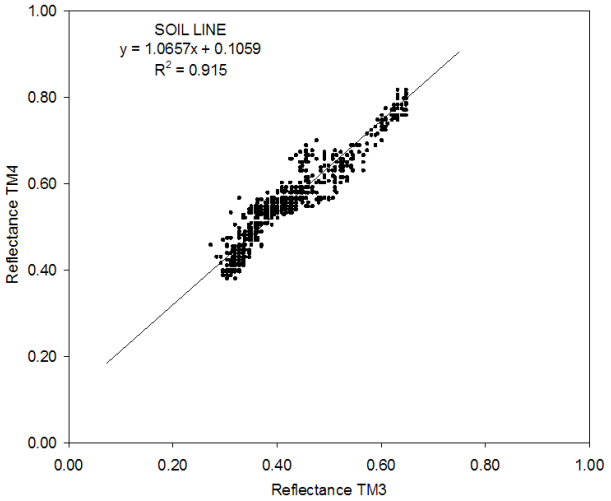

Figure 3. Linear regression analysis for estimating the soil line using reflectance values of TM bands 3 and 4 (1,013 pixels were used for the regression analysis)

The high variability within the soils (in relation to moisture, organic matter content, salinity, etc.) required the sampling of a great number of pixels to capture the different soil variations. A smaller number of pixel sampling may provide a higher correlation coefficient value but will not capture accurately the soil variations found in the study area.

4. Experiment: Statistical Procedure

The computed vegetation indices are presented in Table 1 as classified by the mathematical conceptualization. All the indices were analyzed and tested to determine their potentially redundant information content. Several descriptive values and statistics were computed for all reviewed indices (Table 2).

Table 2. Descriptive values obtained by the application of the indices to the test area

Vegetation Index	Mean	Min.	Max.	Std.dev.	Error
ARVI	0.095	-0.600	0.773	0.131	3.286E-04
B-DTM5	0.280	-0.154	0.734	0.058	1.455E-04
EVI	0.207	-0.111	0.793	0.088	2.207E-04
Greenness	0.089	-0.163	0.556	0.080	2.007E-04
Integral	0.237	0.000	0.45	0.075	1.881E-04
MSARVI	0.009	-0.055	0.07	0.013	3.261E-05
MSI	0.656	0.000	2.000	0.122	3.060E-04
NDII	0.214	-0.333	0.773	0.093	2.333E-04
NDVI	0.282	-0.471	0.844	0.128	3.211E-04
R/G ratio	1.025	0.000	1.458	0.088	2.207E-04
SARVI	0.058	-0.252	0.502	0.080	2.007E-04
SAVI	0.251	-0.185	0.802	0.103	2.584E-04
TSAVI2	0.111	-0.964	0.675	0.114	2.860E-04
Wetness	-0.256	-0.705	0.071	0.094	2.358E-04

For the analysis, 158,938 pixels were used within the study area (and outside the water mask). Mean value, minimum and maximum values, standard deviation, and error (as standard deviation divided by the square root of the number of pixels) were determined for each vegetation index.

For testing the redundant information, a pixel by pixel linear regression analysis was performed on all indices (each index was compared individually against all other indices) in order to evaluate their respective degree of correlation. Slope (a) and correlation coefficient (r^2) parameters of the linear regression analysis were used for testing the redundant information. Slope coefficient indicates the type of relation between two indices. This relation can be direct if the slope coefficient is positive, or it can be indirect if the slope coefficient is negative.

Correlation coefficient (r^2) provides a method to assess the degree of similarity between a pair of variables. A high correlation coefficient value indicates a great degree of similarity between both independent and dependent variables. Correlation coefficients (r^2) vary between 0 and 1. As the correlation coefficient nears to 1, the larger is the similarity between the variables.

Slope (a) and correlation coefficient (r^2) parameters can provide a method of comparison among vegetation indices. Differences in atmospheric effects, vegetation patterns, and other local characteristics can be ignored, because we assume that they have the same effect on all indices. With this assumption, we can estimate if there are potentially redundant information in the selected indices. Linear regression analysis was done for those indices that provide the same kind of vegetation biophysical information. The two groups are: greenness/biomass indices (ARVI, EVI, Greenness, MSARVI, NDVI, SARVI, SAVI, TSAVI2), and vegetation moisture indices (B-D_{TM5}, Integral, MSI, NDII, Wetness). Other third group can be differentiated based on specific vegetation pigment contents. Within this last group, only Red/Green ratio was included.

5. Results of the Experiment

Table 2 provides descriptive values and statistics as obtained from the application of the indices in the test area. Greenness/biomass indices mean values are comprised within the range of 0.009 for MSARVI to 0.282 for NDVI. Vegetation moisture indices mean values are comprised within the range of -0.256 for Wetness to 0.656 for MSI. Error values are low and homogeneous between indices.

DOI: https://doi.org/ 10.30564/jgr.v2i1.499

The lower error value corresponds to MSARVI with an order of magnitude lower than the other indices.

Tables 3 and 4 provide slope (a) and correlation coefficient (r^2) values of greenness/biomass indices for the redundant information test. Slope coefficients are presented in table 3 where independent variables are ordered by columns and dependent variables are ordered by rows. In all cases, slope coefficient values are positive, showing that all greenness/biomass indices have a direct relationship.

Table 3. Slope coefficients (a) of linear regression analysis for greenness/biomass indices

		Slope coefficients of regression lines (a)							
Dependent variables (y)	ARVI		1.44	1.50	10.04	1.01	1.63	1.22	1.09
	EVI	0.64		1.05	6.63	0.64	1.08	0.83	0.76
	Greenness	0.56	0.87		5.86	0.58	0.94	0.76	0.67
	MSARVI	0.10	0.14	0.15		0.10	0.16	0.12	0.11
	NDVI	0.96	1.37	1.50	9.65		1.57	1.20	1.07
	SARVI	0.60	0.89	0.94	6.17	0.61		0.75	0.67
	SAVI	0.76	1.16	1.26	7.81	0.78	1.26		0.90
	TSAVI2	0.81	1.25	1.33	8.23	0.83	1.34	1.07	
		ARVI	EVI	Greenness	MSARVI	NDVI	SARVI	SAVI	TSAVI2
		Independent variables (x)							

Table 4. Correlation coefficients (r^2) of linear regression analysis for greenness/biomass indices

	Correlation coefficients (r2)						
EVI	0.919						
Greenness	0.835	0.914					
MSARVI	0.971	0.949	0.891				
NDVI	0.969	0.877	0.871	0.941			
SARVI	0.987	0.957	0.883	0.992	0.952		
SAVI	0.925	0.967	0.957	0.947	0.941	0.951	
TSAVI2	0.879	0.944	0.895	0.884	0.883	0.893	0.967
	ARVI	EVI	Greenness	MSARVI	NDVI	SARVI	SAVI

The correlation coefficients for greenness/biomass indices are shown in table 4. In general, a high degree of correlation between all selected greenness/biomass indices was found as the number of high correlation coefficients shows (for $r^2 \geq 0.9$). As an example, SAVI is highly correlated with all other selected greenness/biomass indices. EVI is also highly correlated with all other selected greenness/biomass indices except for NDVI. On the contrary, Greenness and TSAVI2 are only highly correlated with EVI and SAVI. ARVI, MSARVI, NDVI and SARVI are highly correlated with 4 or 5 indices. SAVI is the highest correlated index for selected greenness/biomass indices.

Tables 5 and 6 provide slope (a) and correlation coefficient (r^2) values of vegetation moisture indices. Slope coefficients are presented in table 5 where independent variables are ordered by columns and dependent variables are ordered by rows.

Table 5. Slope coefficients (a) of linear regression analysis for vegetation moisture indices

		Slope coefficients of regression lines (a)				
Dependent variables (y)	B-DTM5		-0.15	-0.35	0.46	0.25
	Integral	-0.27		0.40	-0.53	-0.71
	MSI	-1.54	0.97		-1.29	-1.02
	NDII	1.21	-0.76	-0.77		0.79
	Wetness	0.66	-1.06	-0.63	0.82	
		B-DTM5	Integral	MSI	NDII	Wetness
		Independent variables (x)				

Selected vegetation moisture indices show direct or inverse relations as a function of the cross-pair of indices. Therefore, their relation is not as clear as greenness/biomass indices. As an example, MSI shows a direct relation with Integral, and an inverse relation with B-D_{TM5}, NDII, and Wetness. In other case, B-D_{TM5} shows a direct relation with NDII and Wetness, and an inverse relation with Integral and MSI.

Table 6 shows that highly correlated indices (for $r^2 \geq 0.9$) are not frequent within selected vegetation moisture indices. Only MSI and NDII show a high correlation ($r^2 = 0.988$) between them.

Table 6. Correlation coefficients (r^2) of linear regression analysis for vegetation moisture indices

	Correlation coefficients (r2)			
Integral	0.039			
MSI	0.544	0.384		
NDII	0.563	0.402	0.988	
Wetness	0.161	0.755	0.645	0.648
	B-DTM5	Integral	MSI	NDII

6. Conclusion

The great pool of existing vegetation indices provides important tools for vegetation monitoring and analysis. These indices have the potential to be applied as a common tool for agricultural and natural resources management studies. The indices of greenness/biomass, vegetation

 DOI: https://doi.org/ 10.30564/jgr.v2i1.499

moisture, and vegetation pigments content were reviewed and formulated so that they can be easily computed with reflective values of LANDSAT Thematic Mapper (TM) data.

Additionally, a simple method for redundant information testing has been used in order to discriminate similar information contained in these indices. Linear regression analysis has the potential for providing an ubiquitous test, since similar scene conditions are assumed for all computed indices. Detection of direct or inverse relations and the degree of correlation or similarity between indices can be successfully determined.

Although these indices can be grouped according to the purpose for which they were designed and the correlated between them, assuming that they lead to the same biophysical parameter information, several differences have been observed, especially in the magnitude of the values calculated from the reflectance of the bands used. For the area used in this experiment, SAVI appears to be the most appropriate index for greenness/biomass determination although no specific index appears to be the most appropriate in the case of vegetation moisture estimation.

References

[1] Steven, M.D., Malthus, T.J., Baret, F., Xu, H., Chopping, M.J. (2003). Intercalibration of vegetation indices from different sensor systems [C]. Remote Sensing of Environment, 88: 412-422. (https://doi.org/10.1016/j.rse.2003.08.010)

[2] Richardson, A.J., Everitt, J.H. (1992). Using Spectral Vegetation Indices to Estimate Rangeland Productivity [C]. Geocarto International, 1: 63-77. (DOI: 10.1080/10106049209354353)

[3] Lyon, J.G., Yuan, D., Lunetta, R.S., Elvidge, C.D. (1998) A Change Detection Experiment Using Vegetation indices [C]. Photogrammetric Engineering & Remote Sensing, 64, 2: 143-150.

[4] Jensen, J.R. (2000). Remote Sensing of the Environment: An Earth Resource Perspective [M]. Upper Saddle River (NJ), USA: Prentice Hall.

[5] Jensen, J.R. (2004). Introductory Digital Image Processing. A Remote Sensing Perspective. Third edition. [M] Upper Saddle River (NJ), USA: Prentice Hall.

[6] Chuvieco, E., Riaño, D., Aguado, I., Cocero, D. (2002). Estimation of fuel moisture content from multitemporal analysis of Landsat Thematic Mapper reflectance data: applications in fire danger assessment [C]. International Journal of Remote Sensing, 23, 11: 2145-2162. (https://doi.org/10.1080/01431160110069818)

[7] Xue, J., Su, B. (2017). Significant Remote Sensing Vegetation Indices: A Review of Developments and Applications [C]. Journal of Sensors, 2017, Article ID 1353691. (https://doi.org/10.1155/2017/1353691)

[8] Cetin, M., Sevik, H. (2016). Evaluating the recreation potential of Ilgaz Mountain National Park in Turkey [C]. Environmental Monitoring and Assessment, 188, 52. (https://doi.org/10.1007/s10661-015-5064-7)

[9] Potapov, P., Yaroshenko, A., Turubanova, S., Dubinin, M., Laestadius, L., Thies, C., Aksenov, D., Egorov, A., Yesipova, Y., Glushkov, I., Karpachevskiy, M., Kostikova, A., Manisha, A., Tsybikova, E., Zhuravleva, I. (2008). Mapping the World's Intact Forest Landsacapes by Remote Sensing [C]. Ecology and Society, 13, 2: 51. (http://www.ecologyandsociety.org/vol13/iss2/art51/)

[10] Curran, P. (1980). Multiespectral remote sensing of vegetation amount [C]. Progress in Physical Geography: Earth and Environment, 4, 3: 315-341. (https://doi.org/10.1177/030913338000400301)

[11] Running, S.W., Loveland, T.R, Pierce, L.L., Nemani, R.R., Hunt, E.R. Jr. (1995). A Remote Sensing Based Vegetation Classification Logic for Global Land Cover Analysis [C]. Remote Sensing of Environment, 51: 39-48. (https://doi.org/10.1016/0034-4257(94)00063-S)

[12] Estes, J.E., Jensen, J.R., Simonett, D.S. (1980). Impacts of remote sensing on the U.S. Geography [C]. Remote Sensing of Environment, 10: 43-80. (https://doi.org/10.1016/0034-4257(80)90098-X)

[13] Houborga, R., Soegaard, H., Boeghb, E. (2007). Combining vegetation index and model inversion methods for the extraction of key vegetation biophysical parameters using Terra and Aqua MODIS reflectance data [C]. Remote Sensing of Environment, 106, 1: 39-58. (https://doi.org/10.1016/j.rse.2006.07.016)

[14] Jensen, J.R. (1983). Biophysical Remote Sensing. Review Article [C]. Annals of the Association of American Geographers, 73, 1: 111-132. (https://doi.org/10.1111/j.1467-8306.1983.tb01399.x)

[15] Jensen, J.R., Coombs, C., Porter, D., Jones, B., Schill, S., White, D. (1998). Extraction of Smoth Cordgrass (Sparthina alterniflora) Biomass and Leaf Area Index Parameters from High Resolution Imagery [C]. Geocarto International, 13, 4:25-46. (https://doi.org/10.1080/10106049809354661)

[16] Hanna, M.M., Steyn-Ross, D.A., Steyn-Ross, M. (1999). Estimating Biomass for New Zealand Pasture Using Optical Remote Sensing Techniques [C]. Geocarto International, 14, 3: 89-94. (https://doi.org/10.1080/10106049908542121)

[17] Haboudane, D., Miller, J.R., Pattey, E., Zarco-tejada,

DOI: https://doi.org/ 10.30564/jgr.v2i1.499

P., Strachan, I.B. (2004). Hiperespectral vegetation indices and novel algorithms for predicting green LAI of crop canopies: Modelling and validation in the context of precision agriculture [C]. Remote Sensing of Environment, 90: 337-352. (DOI: 10.1016/j.rse.2003.12.013)

[18] Muukkonen, P. & Heiskanen, J. (2005). Estimating biomass for boreal forests using ASTER satellite data combined with standwise forest inventory data [C]. Remote Sensing of Environment, 99, 4: 434-447. (DOI: 10.1016/j.rse.2005.09.011)

[19] Gitelson, A.A. (2004) Wide Dynamic Range Vegetation Index for Remote Quantification of Biophysical Characteristics of Vegetation [C]. Journal of Plant Physiology. 161, 2: 165-173. (https://doi.org/10.1078/0176-1617-01176)

[20] Jackson, R.D. (1982). Canopy temperature and crop water stress [C]. Advances in Irrigation Research, 1: 45-85. (https://doi.org/10.1016/B978-0-12-024301-3.50009-5)

[21] Hunt, E.R., Rock, B.N., Nobel, P.S. (1987). Measurement of Leaf Relative Water Content by Infrared Reflectance [C]. Remote Sensing of Environment, 22: 429-435. (https://doi.org/10.1016/0034-4257(87)90094-0)

[22] Hunt, E.R., Rock, B.N. (1989). Detection of Changes in Leaf Water Content Using Near- and Middle-Infrared Reflectances [C]. Remote Sensing of Environment, 30: 43-54. (https://doi.org/10.1016/0034-4257(89)90046-1)

[23] Gao, B.C. (1996). NDWI. A normalized difference water index for remote sensing of vegetation liquid water from space [C]. Remote Sensing of Environment, 58: 257-266. (https://doi.org/10.1016/S0034-4257(96)00067-3)

[24] Gamon, J.A., Surfus, J.S. (1999). Assessing leaf pigment content and activity with a reflectometer [C]. New Phytologist, 143: 105-117. (https://doi.org/10.1046/j.1469-8137.1999.00424.x)

[25] Gamon, J.A., Serrano, L., Surfus, J.S. (1997). The photochemical reflectance index: an optical indicator of photosynthetic radiation use efficiency across species, function types, and nutrient levels [C]. Acta Oecologica, 112: 492-501. (https://doi.org/10.1007/s004420050337)

[26] Sims, D.A., Gamon, J. (2002). Relationships between leaf pigment content and spectral reflectance across a wide range os species, leaf structures and developmental stages [C]. Remote Sensing of Environment, 81, 2-3: 337-354. (DOI: 10.1016/S0034-4257(02)00010-X)

[27] Schultz, M., Clevers, J.G.P.W., Carter, S., Verbesselt, J., Avitabile, V., Quang, H.V., Herold, M. (2016). Performance of vegetation indices from Landsat time series in deforestation monitoring [C]. International Journal of Applied Earth Observation and Geoinformation, 52: 318-327. (https://doi.org/10.1016/j.jag.2016.06.020)

[28] Huete, A., Justice, C. (1999). MODIS Vegetation Index (MOD 13) Algorithm Theoretical Basis Document. Version 3 [S]. Greenbelt (MD), USA: NASA Goddard Space Flight Center.

[29] Kokaly, R.F., Clark, R.N. (1999). Spectroscopic Determination of Leaf Biochemistry using Band-Depth Analysis of Absorption Features and Stepwise Multiple Linear Regression [C]. Remote Sensing of Environment, 67: 267-287. (https://doi.org/10.1016/S0034-4257(98)00084-4)

[30] Jackson, R.D., Huete, A.R. (1991). Interpreting vegetation indices [C]. Preventive Veterinary Medicine, 11: 185-200. (https://doi.org/10.1016/S0167-5877(05)80004-2)

[31] Eastman, J.R. (2003). IDRISI Kilimanjaro. Guide to GIS and Image Processing [S]. Worcester (MA), USA: Clark University.

[32] Fox, G.A., Sabbagh, G.J. (2002). Estimation of Soil Organic Matter from Red and Near-Infrared Remotely Sensed Data Using a Soil Line Euclidean Distance Technique [C]. Soil Science Society of America Journal, 66, 6: 1922-1929. (DOI:10.2136/sssaj2002.1922)

[33] Clark, R.N., Roush, T.L. (1984). Reflectance spectroscopy: quantitative analysis techniques for remote sensing applications [C]. Journal of Geophysical Research, 89: 6329-6340. (https://doi.org/10.1029/JB089iB07p06329)

[34] Clark, R.N. (1999). Chapter 1: Spectroscopy of Rocks and Minerals, and Principles of Spectroscopy. In: Rencz, A.N. (ed.) [M]. Manual of Remote Sensing, Volume 3, Remote Sensing for the Earth Sciences. New York (USA): John Wiley & Sons, Ltd.: 3-58. (ISBN: 0471-29405-5)

[35] Rouse, J.W., Haas, R.H., Schell, J.A., Deering, D.W. (1974). Monitoring Vegetation Systems in the Great Plains with ERTS [S]. Proceeding, Third Earth Resources Technology Satellite-1 Symposium, NASA SP-351. Goddard Space Flight Center, Greenbelt (MD), USA: 309-317.

[36] Birth, G.S., McVey, G. (1968). Measuring the Color of Growing Turf with a Reflectance Spectrophotometer [C]. Agronomy Journal, 60, 6: 640-643. (DOI: 10.2134/agronj1968.00021962006000060016x)

[37] Deering, D.W., Rouse, J.W., Haas, R.H., Schell, J.A. (1975). Measuring Forage Production of Grazing Units from Landsat MSS data [S]. Proceedings of the

 DOI: https://doi.org/ 10.30564/jgr.v2i1.499

10th International Symposium on Remote Sensing of Environment, ERIM 2. Ann Arrbor, USA: 1169-1178.

[38] Chuvieco, E. (2002). Teledetección ambiental. La observación de la Tierra desde el espacio [M]. Barcelona (Spain): Ariel Ciencia. (ISBN: 8434480727)

[39] Rondeaux, G., Steven, M., Baret, F. (1996) Optimization of Soil-Adjusted Vegetation Indices [C]. Remote Sensing of Environment, 55: 95-107. (https://doi.org/10.1016/0034-4257(95)00186-7)

[40] Verhoef, W. (1984). Light scattering by leaf layers with application to canopy reflectance modelling: the SAIL model [C]. Remote Sensing of Environment, 16, 2: 125-141. (https://doi.org/10.1016/0034-4257(84)90057-9)

[41] Kuusk, A. (1991). The hot-spot effect in plant caopy reflectance [M]. In R.B. Myneni and J. Ross Eds.), Photon-Vegetation interactions, Application in Optical Remote Sensing and Plant Ecology. New York: Springer Verlag.: 139-159. (DOI: 10.1007/978-3-642-75389-3_5)

[42] Huete, A.R. (1988) A Soil Adjusted Vegetation Index (SAVI) [C]. Remote Sensing of Environment, 25, 3: 295-309. (https://doi.org/10.1016/0034-4257(88)90106-X)

[43] Huete, A.R., Hua, G., Qi, J., Chehbouni, A., Van Leeuwem, W.J. (1992). Normalization of Multidirectional Red and Near-Infrared Reflectances with the SAVI [C]. Remote Sensing of Environment, 41, 2-3: 143-154. (https://doi.org/10.1016/0034-4257(92)90074-T)

[44] Steven, M.D. (1998). The sensitivity of the OSAVI vegetation index to observational parameters [C]. Remote Sensing of Environment, 63, 1: 49-60. (https://doi.org/10.1016/S0034-4257(97)00114-4)

[45] Kaufman, Y.J., Tanre, D. (1992). Atmospherically Resistant Vegetation index (ARVI) for EOS-MODIS [C]. IEEE Transactions on Geosciences and Remote Sensing, 30, 2: 261-270. (DOI: 10.1109/36.134076)

[46] Hardisky, M.A., Klemas, V., Smart, M. (1983). The Influence of Soil Salinity, Growth From, and Leaf Moisture on the Spectral Radiance of Spartina alternifolia Canopies [C]. Photogrammetric Engineering and Remote Sensing, 49, 1: 77-83. (DOI: 0099-1112183/4901-77$02.25/0)

[47] Carter, G. (1991). Primary and Secondary Effects of Water Content on the Spectral Reflectance of Leaves [C]. American Journal of Botany, 78, 7: 916-924. (https://doi.org/10.1002/j.1537-2197.1991.tb14495.x)

[48] Ceccato, P., Flasse, S., Tarantola, S., Jacquemound, S., Grégoire, J.M. (2001). Detecting vegetation leaf water content using reflectance in the optical domain [C]. Remote Sensing of Environment, 77, 1: 22-33. (https://doi.org/10.1016/S0034-4257(01)00191-2)

[49] Gould, K.S., Kuhn, D.N., Lee, D.W., Oberbauer, S.F. (1995). Why leaves are sometimes red [S]. Nature, 378, 6554: 241-242. (DOI: 10.1038/378241b0)

[50] Coley, P.D., Aide, T.M., (1989). Red coloration of tropical young leaves: a possible anti-fungal defence? [C]. Journal of Tropical Ecology, 5, 03: 293-300. (DOI: 10.1017/S0266467400003667)

[51] Coley, P.D., Barone, J.A. (1996). Herbivory and plant defenses in tropical forest [C]. Annual Review of Ecology and Systematics, 27: 305-335. (https://doi.org/10.1146/annurev.ecolsys.27.1.305)

[52] Qi, J., Chehbouni, Al, Huete, A.R., Kerr, Y.H., Sorooshian, S. (1994). A modified soil adjusted vegetation index (MSAVI) [C]. Remote Sensing of Environment, 48, 2: 119-126. (DOI: 10.1016/0034-4257(94)90134-1)

[53] Richardson, A.J., Wiegand, C.L. (1977). Distinguishing vegetation from soil background information [C]. Photogrammetric Engineering & Remote Sensing, 43, 12: 1541-1552. (ISSN: 0099-1112)

[54] Fox, G.A., Sabbagh, G.J., Searcy, S.W., Yang, C. (2004). An Automated Soil Line Identification Routine for Remotely Sensed Images [C]. Soil Science Society of America Journal, 68, 4: 1326-1331. (DOI: 10.2136/sssaj2004.1326)

[55] Clevers, J.G.P.W. (1988). The derivation of a simplified reflectance model for the estimation of leaf area index [C]. Remote Sensing of Environment, 25, 1: 53-69. (https://doi.org/10.1016/0034-4257(88)90041-7)

[56] Clevers, J.G.P.W., Verhoef, W. (1993). LAI estimation by means of the WDVI: A sensitivity analysis with a combined PROSPECT-SAIL model [C]. Remote Sensing Reviews, 7, 1: 43-64. (DOI: 10.1080/02757259309532165)

[57] Baret, F., Guyot, G.; Major, D. (1989). TSAVI: A Vegetation Index Which Minimizes Soil Brightness Effects on LAI and APAR Estimation [S]. 12th Canadian Symposium on Remote Sensing and IGARSS'90. Volume 4. Vancouver, Canada.: 10-14. (DOI: 10.1109/IGARSS.1989.576128)

[58] Gilabert, M.A., González-Piqueras, J., García-Haro, F.J., Meliá, J. (2002). A generalizad soil-adjusted vegetation index [C]. Remote Sensing of Environment, 82, 2-3: 303-310. (https://doi.org/10.1016/S0034-4257(02)00048-2)

[59] Huete, A.R., Liu, H.Q. (1994). An Error and Sensitivity Analysis of the Atmospheric- and Soil-Correcting Variants of the Normalized Difference Vegetation Index for the MODIS-EOS [C]. IEEE Transactions

on Geosciences and Remote Sensing, 32, 4: 897-905. (DOI: 10.1109/36.298018)

[60] Kauth, R.J., Thomas, G.S. (1976). The Tasseled Cap: A Graphic Description of the Spectral Temporal Development of Agricultural Crops as Seen By Landsat [S]. In Proceedings, Machine Processing of Remotely Sensed Data. Laboratory for the Applications of Remote Sensing (LARS), Purdue University, West Lafayette (IN), USA: 41-51. (http://docs.lib.purdue.edu/lars_symp/159)

[61] Crist, E.P. (1985). A Thematic Mapper Tasseled Cap Equivalent for Reflectance Factor Data [C]. Remote Sensing of Environment, 17, 3: 301-306. (https://doi.org/10.1016/0034-4257(85)90102-6)

[62] Crist, E.P. (1983). The TM tasselled cap: A preliminary formulation [S]. In Proceedings of the Symposium on Machine Processing of Remotely Sensed Data. Laboratory for the Applications of Remote Sensing (LARS), Purdue University, West Lafayette (IN), USA: 357-364.

[63] Crist, E.P., Cicone, R.C. (1984a). Comparison of the dimensionality and features of simulated Landsat-4 MSS and TM data [C]. Remote Sensing of Environment, 14, 1-3: 235-246. (https://doi.org/10.1016/0034-4257(84)90018-X)

[64] Crist, E.P., Cicone, R.C. (1984b). A physically-based transformation of thematic mapper data – the TM Tasseled Cap [C]. IEEE Transactions on Geoscience and Remote Sensing, 22, 3: 256-263. (DOI: 10.1109/TGRS.1984.350619)

[65] Crist, E.P., Kauth, (1986). The Tasselled Cap de-mystified [C]. Photogrammetric Engineering and Remote Sensing, 52, 1: 81-86. (DOI: 0099-1112186/5201-0081$02.25/0)

[66] Jackson, R.D. (1983). Spectral Indices in n-Space [C]. Remote Sensing of Environment, 13, 5: 409-421. (https://doi.org/10.1016/0034-4257(83)90010-X)

[67] Clark, R.N., Roush, T.L. (1984). Reflectance spectroscopy: quantitative analysis techniques for remote sensing applications [C]. Journal of Geophysical Research, 89, B7: 6329-6340. (DOI: 10.1029/JB089iB07p06329)

[68] Clark, R.N. (1999). Chapter 1: Spectroscopy of Rocks and Minerals, and Principles of Spectroscopy [M]. In: Rencz, A.N. (ed.). Manual of Remote Sensing, Volume 3, Remote Sensing for the Earth Sciences. New York (USA): John Wiley & Sons, Ltd.: 3-58.

[69] Clark, R. N., Swayze, G. A., Livo, K. E., Kokaly, R. F., Sutley, S. J., Dalton, J. B., McDougal, R. R., Gent, C. A. (2003). Imaging Spectroscopy: Earth and Planetary Remote Sensing with the USGS Tetracorder and Expert Systems [C]. Journal of Geophysical Research, 108, E12: 5131. (DOI: 10.1029/2002JE001847.v)

[70] Van Niel, T.G., McVicar, T.R., Fang, H., Liang, S. (2003). Calculating environmental moisture for per-field discrimination of rice crops [C]. International Journal of Remote Sensing, 24, 4: 885-890. (DOI: 10.1080/0143116021000009921)

[71] Mather, P.M. (2004). Computer Processing of Remotely-Sensed Images. An Introduction [M]. Third edition. West Sussex (England), UK: John Wiley & Sons, Ltd. (ISBN: 9780470849187)

[72] Chander, G., Markham, B. (2003). Revised Landsat-5 TM radiometric calibration procedures and post-calibration dynamic ranges [R]. IEEE Transactions of Geosciences and Remote Sensing, 41, 11: 2674-2677. (DOI: 10.1109/TGRS.2003.818464)

[73] Chavez, P. (1988). An improved dark-object subtraction technique for atmospheric scattering correction of multispectral data [C]. Remote Sensing of Environment, 24, 3: 459-479. (https://doi.org/10.1016/0034-4257(88)90019-3)

[74] Koch, M. (2000). Geological controls of land degradation as detected by remote sensing: a case study in Los Monegros, north-east Spain [C]. International Journal of Remote Sensing, 21, 3: 457-473. (DOI: 10.1080/014311600210687)

[75] Dewa, R.P., Danoedoro, P. (2017). The effect of image radiometric correction on the accuracy of vegetation canopy density estimate using several Landsat-8 OLI's vegetation indices: A case study of Wonosari area, Indonesia [S]. IOP Conference Series: Earth and Environmental Science, 54, 012046. (DOI: 10.1088/1755-1315/54/1/012046)

[76] Hoffer, R.M. (1978). Biological and physical considerations in applying computer-aided analysis techniques to remote sensor data. In Swain, P.H. and Davis, S.M. (eds.), Remote Sensing: The Quantitative Approach, McGraw- Hill Book Company, New York: 227-289.